HEFAT2008
6th International Conference on Heat Transfer, Fluid Mechanics and Thermodynamics
30 June to 2 July 2008
Pretoria, South Africa
Paper number: HT1

INFLUENCE OF ASYMMETRIC BLOCKAGE AT FLOW EXIT ON FLOW AND HEAT TRANSFER FOR AN IMPINGING SLOT JET ON SEMI-CONCAVE SURFACE

Hoang T.K.D.[1,2]*, Brizzi L.E.[1], Dorignac E.[2] and Fénot M.[2]
*Author for correspondence
[1] Laboratoire d'Etudes Aérodynamiques - SP2MI,
Futuroscope Chasseneuil Cedex, 86962,
France
[2] Laboratoire d'Etudes Thermiques – ENSMA,
Futuroscope Chasseneuil Cedex, 86961,
France
E-mail: dung.hoang@lea.univ-poitiers.fr

ABSTRACT

Experimental studies of single slot jet impinging upon a concave surface are conducted by classical **P**article **I**mage **V**elocimetry (PIV) and infrared thermography, with nozzle exit Reynolds number (Re = 3200), dimensionless impinging height (H/b = 3 & 7) and relative curvature of the wall (Dc/b = 5). Results indicate that the oscillatory impinging jet generated a uniform and symmetric heat transfer area while the stabilized impinging jet caused an asymmetric heat transfer. This type of jet may be controlled by changing the outlet condition.

NOMENCLATURE

b	[mm]	Width of the slot
Dc	[mm]	Diameter of concave wall
e	[mm]	Outlet spacing
H	[mm]	Impinging height
h	[W/m^{2}K]	Local heat transfer coefficient
k	[W/mK]	Thermal conductivity
Nu	[-]	Nusselt number ($h.b/k_{air}$)
Re	[-]	Nozzle exit Reynolds number ($U_j.b/\nu$)
RMS	[m/s]	Mean root-mean-square ($(u'^2 + v'^2)^{1/2}$)
S	[mm]	Curvilinear coordinate
U, V	[m/s]	Streamwise, transverse mean velocity
u', v'	[m/s]	Streamwise, transverse RMS velocity fluctuation
X,Y,Z	[mm]	Streamwise, transverse and spanwise coordinates
$\overline{Nu}$	[-]	Average Nusselt number

Special characters

υ	[m^2/s]	Kinetic viscosity

Subscripts

air	Relative to air
j	Injection

INTRODUCTION

Air jets provide an effective mean for cooling surfaces of various geometries. Jet dynamics and flow structures must be studied to understand and optimize the heat transfer obtained with impinging jet. Most of the studies on jets have focused on impingement on flat surfaces because of their strong potential concerning thermal transfers. Recently, the interest moved on impingement with the presence of curved (convex/concave) surfaces. Indeed, the exact role of the curvature on the transfer of mass and/or heat are still unknown. To approach this problem, we have undertaken for the past few years, aero-thermal studies on the flow generated by impinging one or more jets on a concave surface.

Using particle image velocimetry (PIV), Gilard & Brizzi [1] have noted the presence of three semi-stable flow regimes in the vicinity of the concave wall at large dimensionless impinging height. These regimes were found to generate a uniform heat transfer for an impinging slot jet on a flat plate (numeric study [2]). At small dimensionless impinging heights, the impinging jet stabilizes at the center of the concave wall. According to Yang & al. [3], the thermal transfer is maximal at the stagnation point and corresponds to the location of maximum turbulence intensity.

Moreover, Hoang & al. [4] notice that the oscillation of impinging jet observed in [1] is controllable by varying the outlet condition. A flow recirculation is observed and is appreciably changed with the outlet condition. Kornblum & Goldstein [5] suggested that this recirculation would cause an increase in fluid temperature close to the wall. The heat transfer coefficient being calculated from nozzle exit temperature, this rise in jet temperature would cause a drop of heat transfer. Kornblum & Goldstein [5] also noted that the impinging height has an important role to play on the jet structure. At the small spacing, the jet velocity is still high; it mixes significantly with the entrained air, and induces

turbulence and eddy activity, all of which enhance h, hence its maximum value.

Interest of all authors quoted above concerns the impact of single slot jet on a curved wall (concave/convexes). In order to use this kind of jet to optimize the cooling of a concave surface, we propose to study in this paper the effect of the outlet condition by using an obturator (colored zone in figure 1a). The dynamics and structure of an impinging slot jet will be encountered by using classical PIV, and an infrared thermography will be used to carry out the thermal transfer.

EXPERIMENTAL APPARATUS

Experimental set-up

The impinging slot jet is supplied by a right-angled parallelepiped channel (955mm length, 300mm width and 10mm height). A grid and a honeycomb are placed upstream in order to make the flow uniform.

The impingement surface consists of two parts: One is a semi-cylindrical shape (450mm length and 50mm diameter) and corresponds to the curved part of the impingement surface; the other is straight (450mm length and 140mm width) in order to avoid external disturbances which would contaminate the jet (Figure 1a). The impingement surface is closed laterally by transparent plates (thickness of 10mm). All these elements are transparent (Altuglas 3mm thick) in order to do measurements by classical PIV velocimetry or heating plate are used (epoxy/copper 0.2mm thick, whose thermal conductivity is 0.29±0.02W/mK in thick direction) to allow for thermal measurements (heat thin foil technique, infrared thermography). The concave surface is fixed on a moving system making it possible to vary the impinging height H (H is the distance between nozzle exit and the center of the impingement surface).

This testing apparatus comprises of an air feed system established by a fan F 802 (2m^3/min under 1000mm EC, 3.9kW, 2910tr/min) or a centrifugal fan HP APE 801C (3m^3/min, 11368Pa, 5.3kW, 2900tr/min) respectively corresponding to dynamic and thermal measurements.

For the dynamic measurements, air flow rate Qj is controlled using manual valves and three different Fischer & Porter flowmeters connected in parallel. These flowmeters have different measurement ranges in order to optimize the accuracy of the aerodynamic measurements. For thermal measurements, the air flow rate is measured by a venturi meter. The venturi is equipped with two pressure sensors (a differential pressure (0-5mbar) and a static pressure (800-1200mbar)) and a thermocouple (chromel/alumel) to measure the fluid temperature in the venturi. The temperature is controlled by a heat exchanger placed between the flowmeters and the channel. Finally, all elements of this feeding system (fan, valves, flowmeters and thermal regulator) are integrated using PVC pipes or flexible 80 mm diameter plastic tubes. The feeding system is connected to the channel by a diffuser.

In this paper, the main experimental parameters are the nozzle exit Reynolds number Re=3200, the dimensionless impinging height H/b=3&7, and the relative curvature Dc/b=5. The aim of this work is to study the influence of asymmetric blockage at the exit on the flow and heat transfer for an impinging slot jet. One of the simplest means to reach that goal is the use of an obturator. The outlet condition is obtained using an obturator at the right exit of the impact surface (Figure 1). The spacing of this obstruction will be adjustable from 0 to 10 mm. Consequently, e=0mm corresponds to a total obstruction of the right exit while e=10mm presents a maximum opening.

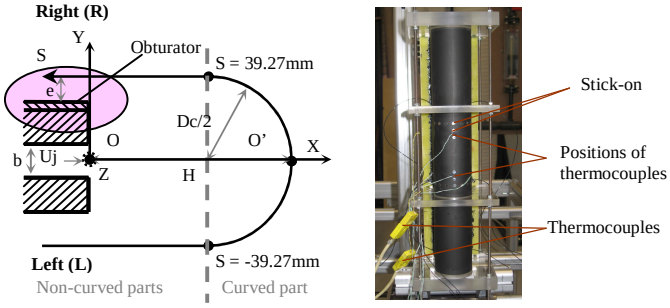

a – Outlet condition (colored zone) b – Impinging surface

Figure 1 Experimental setup

Classical PIV

The velocity was measured by using particle image velocimetry technique (LAVISION technology). An Nd-Yag double cavity QUANTEL laser source (2*120mJ, 10Hz and 532nm) is used to illuminate the flow with a relatively fine luminous plan (≈1.5mm). Flow is seeded by using a generator of olive oil droplets (average diameter ≈1µm).

Pictures are taken using Flowmaster CCD camera (12bits, 1376x1040pixels^2 double frames, 4-5Hz). The recorded images are analyzed in order to obtain displacement of tracers, and then velocity. For this treatment, we use a multipass inter-correlation (4 passes, the last being doubled, started with 128x128 and finish with 32x32), with an overlap of 50%x50%.

As a first step, in order to minimize the influence of reflections or other artifacts, a "basic image" is subtracted from each image before the computation of vectors. This "basic image" is obtained before recording sequences under the same experimental measurements conditions but in absence of particles.

Measurements are obtained for several experimental configurations. For each configuration, 5000 independent samples of measurements are recorded at 4-5Hz, divided into 25 packages of 200 recordings. For the instantaneous fields, different validation and statistical processes are implemented to obtain mean velocity (U, V) and Reynolds stresses ($\sqrt{u'^2}$, $\sqrt{v'^2}$, $u'v'$) values. However for areas where there are less than 1000 validated vectors, no result is presented.

Infrared thermography

Infrared thermography combines the advantage of being no-intrusive and allows for continuous measurements on the surface. This technique is carried out with an infrared matrix camera CEDIP Jade MWIR (InSb, 3.6-5.1µm,

320x240pixels) and a CEDIP infrared system (Altaïr&Saphir). The infrared camera counts the photons, converts them into electric power (V) and then digitizes the signal (DL) to finally transform these results into temperature field (K) through calibration data. The data frequency remains 50 Hz, and a series of images is recorded using Altaïr software for 10 seconds intervals (500 images), and then an average is calculated by the SAPHIR software. From acquisitions of 5 different fluxes, convective heat transfer coefficient h is calculated according to a linear regression method [6]. The values of h are obtained with an accuracy of ±12%.

Averaged Nusselt number is then obtained by integrating local Nusselt numbers over the cylinder surface as

$$\overline{Nu} = \frac{1}{S_2 - S_1} \int_{S_1}^{S_2} Nu \cdot dS \qquad (1)$$

where S_1 & S_2 are limits of the electrical heating circuit, so S_1=-70mm and S_2=70mm.

For the heat thin foil technique, the impingement side (front side) of the heating plate is covered by a fine layer of copper (0.35µm thick). Three individual electric circuits are printed on this side, which heats up the impingement plate by Joule effect. The width of the copper track is 1mm and the inter-track is 0.2mm. These dimensions ensure a uniform heat flux density on the entire front surface of the impingement plate within ±5% of the mean heat flux density over all the electric circuits [7].

Although reflective stick-on (Figure 1.b) allows for a precise location, the change of position of the camera involves an uncertainty on curvilinear coordinates (±1mm).

The ambient temperature was encountered by averaging temperature measurement of two thermocouples chromel/alumel.

RESULTS

According to Gilard & Brizzi [1], for a dimensionless impinging height of H/b=3, the air slot jet hits the center of the concave wall (X=30mm and Y/b=0), then separates in two parts. The maximum intensity fluctuations is close to the stagnation point. This behavior is similar to the one observed by Yang & al. [3]. However, for H/b=7, Gilard & Brizzi [1] noted that this stabilized jet is not found. The air slot jet oscillates at three different semi-stable points. This oscillation phenomenon has a strong effect on local heat transfer [2] and can be controlled by changing the spacing of the outlet [4]. To better understand these jet behaviors and the effect of the outlet condition, we first present the stabilized jet for H/b=3, then the oscillatory impinging jet for H/b=7 will be discussed.

Impinging jet – stabilization

Figure 2 presents the streamlines and the RMS values obtained at different outlet spacing for the following parameters (Re=3200, H/b=3).

Whatever the value of e, the air impinging jet always impacts the concave surface, then separates in two parts like the phenomenon observed in [1], [3]. The location of this stagnation point changes appreciably with the outlet spacing. This stagnation point is further away from the center of the concave surface for e=0, and progresses to the point (X=30mm and Y=0) when e increases from 0 to 10mm [4].

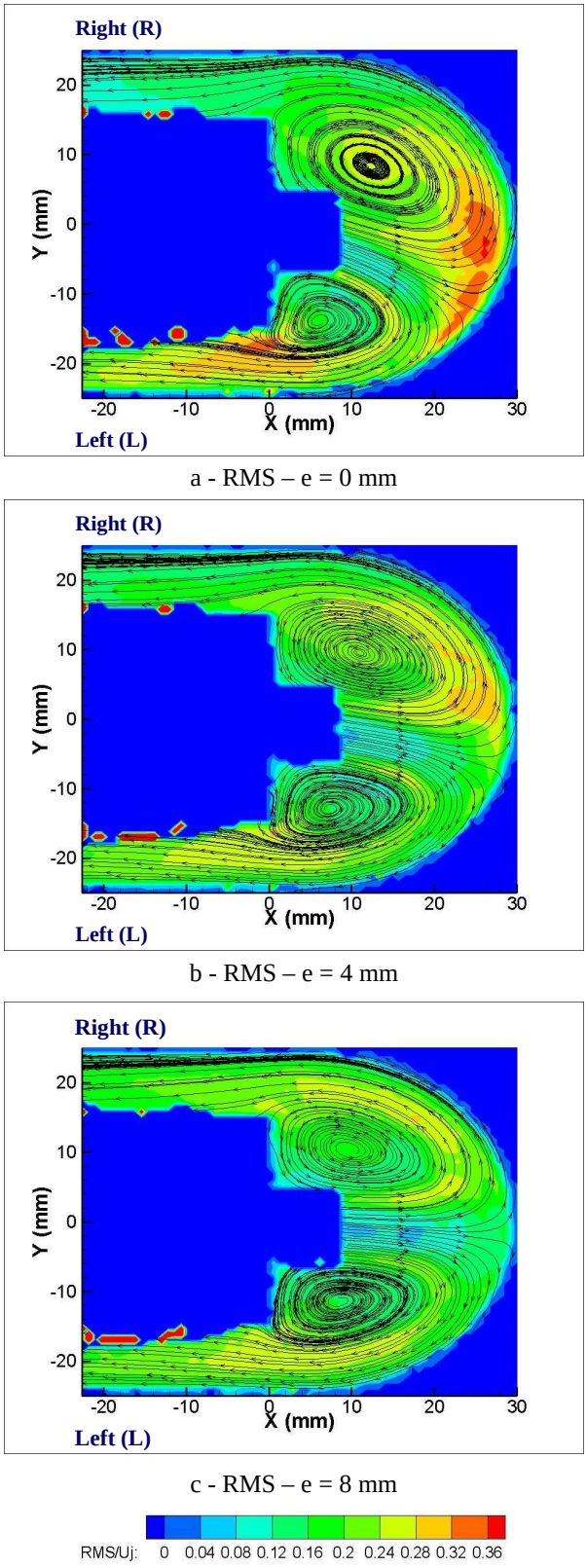

a - RMS – e = 0 mm

b - RMS – e = 4 mm

c - RMS – e = 8 mm

Figure 2 Streamlines and RMS values (Re = 3200; H/b = 3)

We can notice that, when one part of the exit flow is blocked, the flow must go back and consequently, affects jet structure. This enhances the turbulence intensity in the vicinity of stagnation point. Therefore, as e decreases, important intensity turbulence levels are encountered along with a dominant exit flow at the non-blocked part.

At e=10mm, we observe a symmetric thermal transfer with a maximum Nusselt number at the stagnation point [2], [3], [5]. This symmetry becomes asymmetric when the outlet spacing is changed. A peak local Nusselt number is always observed, which corresponds to the location of the stagnation point (Figure 3). This peak value reduces with increase outlet spacing and it depends mainly on the location of the stagnation point. If the stagnation point is closer to the non-blocked (left) exit, the jet velocity at this point is higher where it mixes significantly with the entrained air and induces turbulence and eddy activity, all of which enhance Nu.

We can notice that the Nu number value at the left part is always higher than the Nu number value at the right part because of the dominating exit flow at the left part. This behavior of Nu number tends toward a symmetrical profile when the outlet spacing increases to 10mm.

The average Nusselt number $\overline{Nu}$, regardless of the value of e (e=0 to 10mm) is 24±0.5. Consequently, the asymmetric blockage at the flow exit has a strong effect locally but it has no effect in average.

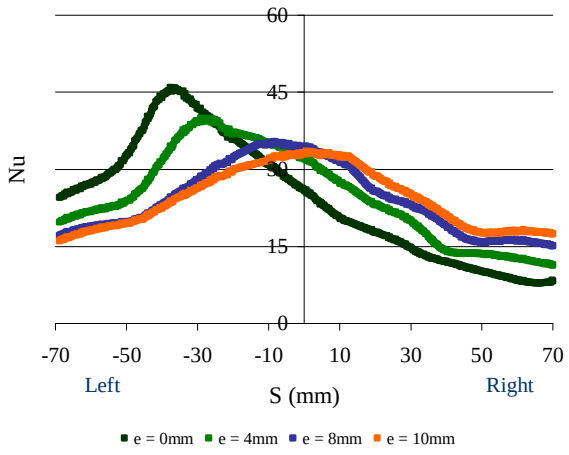

Figure 3 Circumferential Nusselt number distribution (Re=3200; H/b=3)

Impinging jet – oscillation

Figure 4 shows the streamlines and RMS values obtained by classical PIV for case (Re=3200; H/b=7). We observe now two kinds of impact: stabilized (Figure 4 a, b & c) and oscillatory impinging jet (Figure 4 d, e & f). The smaller outlet spacing (e=0; 2 & 4mm) causes a stabilized jet at the non-blocked part of the concave surface, while the impinging jet oscillates around three semi-stable points when the right exit is mainly opened (e=6; 8 & 10mm) [4].

For e=0mm (Figure 4a), the jet stabilizes at a point (X=12mm; Y=-25mm) close to the left exit of the wall with a turbulence intensity ≈ $0.3U_j$; and a 3rd vortex (zone A, Figure 4a) is observed at the blocked (right) part. This stabilization presents a maximum heat transfer while the 3rd vortex causes a minimum heat transfer (Figure 5).

At e=10mm (Figure 4f), the jet does not hit directly on the center of the concave wall, but oscillates three semi-stable points (X=70mm; Y=0 and X=45mm; Y=±25mm). Two zones with high turbulence intensity (≈$0.6U_j$) are located symmetrically about the jet axis in X=45mm and Y=±25mm [1]. For this condition, the local Nusselt number distribution is uniform and symmetric according to the jet axis Y=0. The Nu number value in the straight part of the concave wall are higher than the Nu number value in the curved part because the jet impinges more frequently at two points in the straight parts (X=45mm; Y=±25mm) than at the center of the curved part (X=70mm; Y=0mm).

For the streamlines in Figure 4, we observe that the location of the stagnation point on the mean flow field progresses to the center of the concave surface when the outlet spacing e increases from 0 to 10mm. The structure of jet and heat transfer distribution (Figure 4 and 5) become symmetric with the increase of the obstruction spacing at the outlet up to e=10mm.

The turbulence intensity level of the stabilized jet (≈$0.3U_j$) is always lower than to the oscillatory jet (≈$0.6U_j$). However, the Nusselt number in the non-blocked part of the wall for the stabilized impinging jet case is higher than for the oscillatory impinging jet case. It should be a function of the characteristic of the impact jet at the surface. The stabilized impact leads to a maximum heat transfer at the stagnation point (cf. impinging jet – stabilization), and the oscillation at three semi-stable points generates a uniform heat transfer.

The Nu number value of the blocked (right) part is always lower than the Nu number value at the other part because of the greater exit flow at the non-blocked part. According to Hoang & al. [4], a flow recirculation is clearly presented at the blocked part of the wall at e = 0 and then reduces with the increase spacing at the outlet. This flow recirculation explains the drop of local Nusselt number we observed on figure 5 [5].

For the stabilized jet case (e=0 to 4mm), only one zone with high turbulence intensity (≈$0.3U_j$) is found at the vicinity of the stagnation point, and a maximum heat transfer is also present at this location. The flow recirculation appears earlier than for the case of oscillatory impinging jet.

For the oscillatory impinging jet (e=6 to 10mm), two zones with high turbulence intensity (≈$0.6U_j$) are observed. The jet dynamics and the heat transfer in this case are not to different for the two parts (blocked/non-blocked). We can not observe the flow recirculation at the blocked part similar to the case of stabilized jet. It should be due to the fact that, either the flow recirculation is not present for this case (the recirculation is reduced to a minimum), or the experimental impinging surface is not large enough to observe this kind of flow.

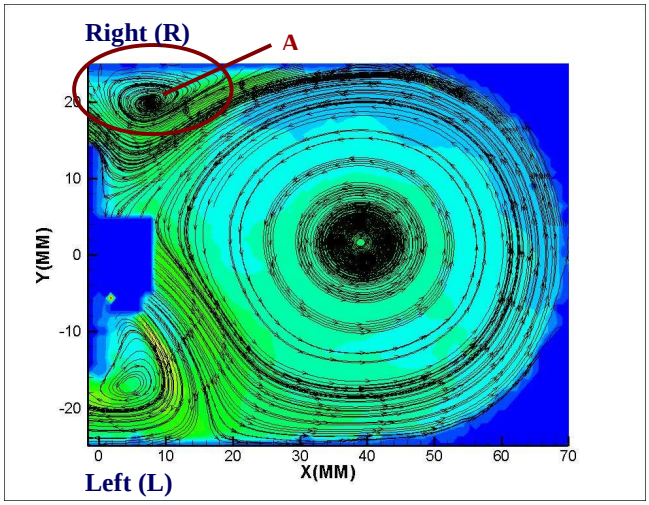

a – e = 0 mm

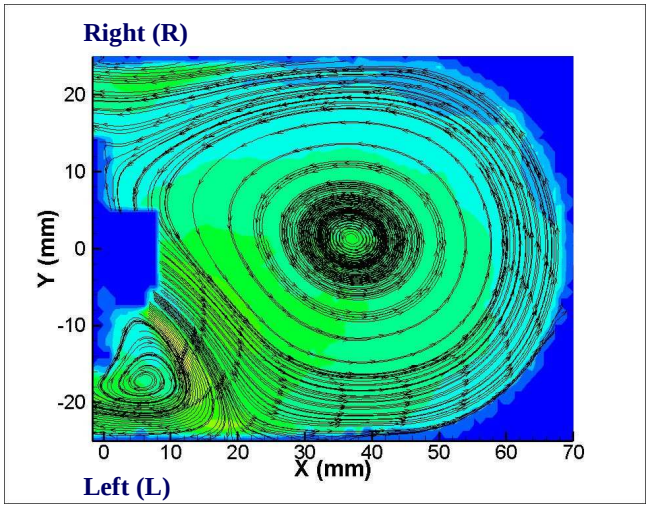

b – e = 2 mm

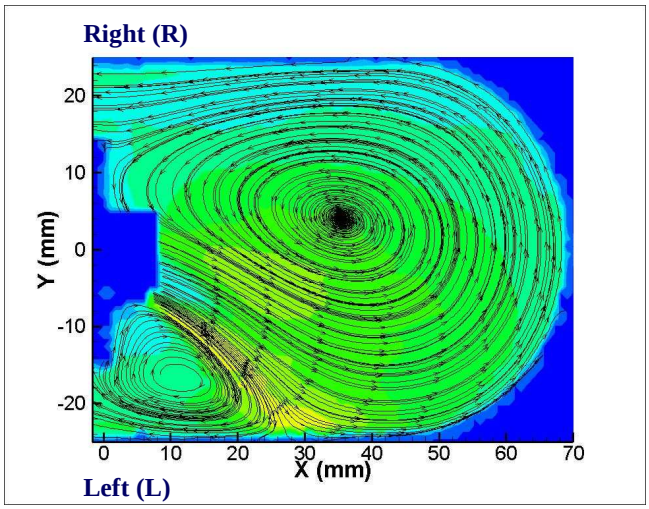

c – e = 4 mm

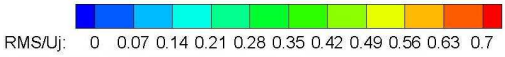

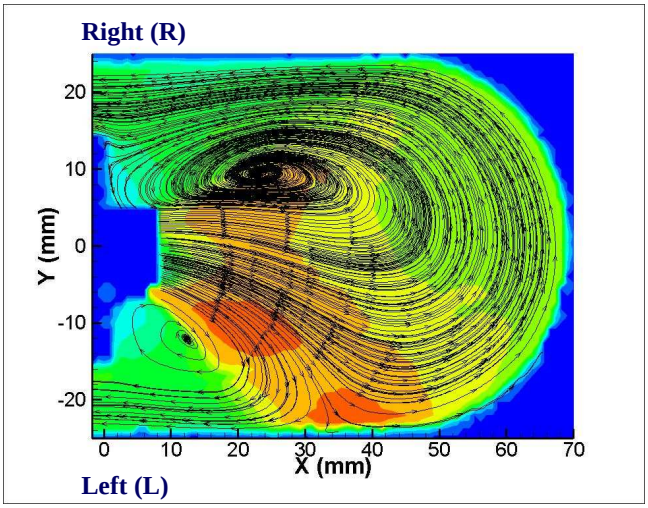

d – e = 6 mm

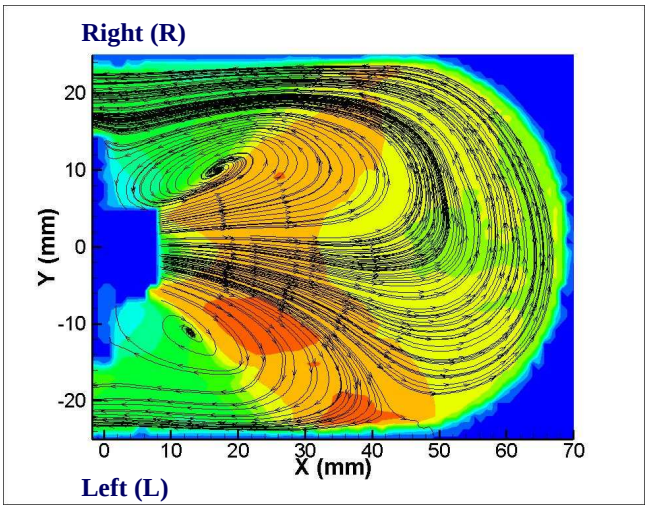

e – e = 8 mm

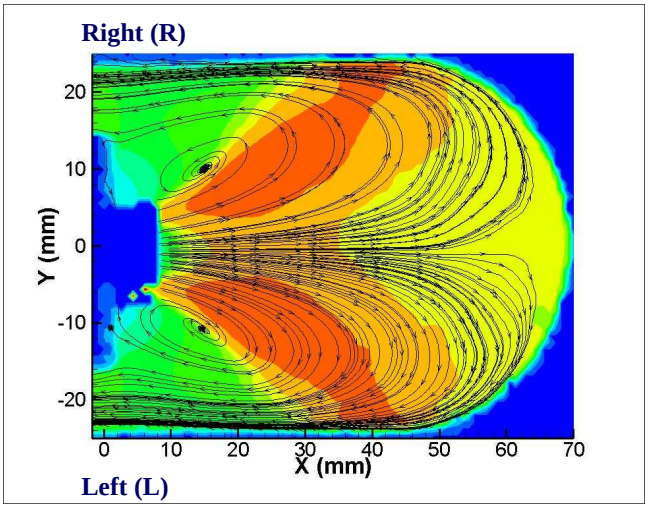

f – e = 10 mm

Figure 4 Streamlines and RMS values (Re_b = 3200; H/b = 7)

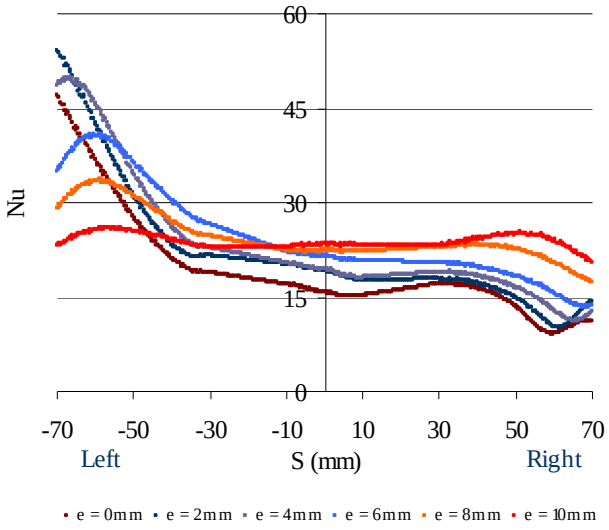

Figure 5 Circumferential Nusselt number distribution (Re=3200; H/b=7)

Table 1 presents the average Nusselt number $\overline{Nu}$ for different outlet spacing (e): the average Nusselt number is rather constant for e=6 to 10mm (≈24±0.5), but for e=0 to 4mm, these $\overline{Nu}$ values are smaller. The heating plate dimension could explain this difference. Indeed, we think that its straight length is not sufficiently large to observe correctly the local Nusselt number distribution for these cases (e=0 to 4mm). The maximum value of Nu number for these cases is located outside or near the physical limit of the thermal experimental set-up, in particular these maximum values of Nu number are not visible (Figure 5) which lead to the smaller $\overline{Nu}$ values.

	0	2	4	6	8	10
$\overline{Nu}$	(19.4)	(22.1)	(23.3)	24.5	24.5	24

Table 1 Average Nusselt number for different e (Re=3200; H/b=7)

Comparison

At H/b=3 and e=10mm, the local Nusselt number is maximum at the stagnation point and its value is about 33. At H/b=7 and e=10mm, heat transfer is nearly constant (Nu≈24). Thus, the oscillatory impinging jet suppresses the maximum heat transfer and the impinging height has an important role to play on the impinging jet. The heat transfer increases when the dimensionless impinging height falls to e=10mm. However, for different outlet spacing (e=0 to 4 mm, stabilized jet), the maximum value of Nu number for the case H/b=7 is always higher than the maximum value of Nu number for the case H/b=3, which is an opposite behavior to the one observed for e=10mm. This difference seems to be due to both the effect of the outlet spacing and also to the influence of impinging height.

The average Nusselt number $\overline{Nu}$ for symmetric exit flow (e=10mm) at Re=3200 is the same for H/b=3 and H/b=7 and is about 24±0.5.

Moreover, the flow recirculation is clearly observed only at the maximum height (H/b=7). This is because of the location of the obturator. The axial distance between the nozzle exit plan and the extremity of the straight portion of concave surface is 40mm higher for the H/b=3 case than for the H/b=7 case. It seems that, at smaller height, the flow goes out through the blocked part. Indeed, this part is moderately affected by the return flow.

CONCLUSION

Through experimental study for single slot impinging jet on a concave surface, we can summarize our main conclusions as follows:

✓ The lower the dimensionless impinging height is, the higher the heat transfer. The dimensionless impinging height plays an important role on impinging jet. At H/b = 3, the jet stabilizes at a point where a maximum heat transfer is found. For H/b=7 where we observe the oscillation of impinging jet, no maximum heat transfer is noticeable. This oscillation creates a uniform heat transfer distribution. It should be noted that the maximum heat transfer at the stagnation point characterizes the stabilized impinging jet. On the other side, the uniformity of the heat transfer is related to the oscillatory impinging jet.

✓ The outlet condition has an important effect on both stabilized and oscillatory impinging jets. This boundary condition is interesting to understand and optimizes only the local heat transfer on a concave surface but not the average heat transfer.

REFERENCES

[1] Gilard V., and Brizzi L.E., Slot jet impinging on a concave curved wall, *Journal of Fluids Engineering*, Vol. 127, No. 3, 2005, pp. 595-603

[2] Suh Y.K., Park J.H., Jeon E.C., and Kim J.W., A numerical study on the oscillotory impinging jet, *SAE 2004 Word Congress & Exhibition*, 2004

[3] Yang G., Choi M., and Lee J.S., An experimental study of slot jet impingement cooling on concave surface: effects of nozzle configuration and curvature, *International Journal of Heat and Mass Transfer*, Vol. 42, 1999, pp. 2199-2209

[4] Hoang T.K.D, Brizzi L.E., and Dorignac E., Influence des conditions d'entrée/sortie pour un jet plan impactant une surface concave en milieu confiné, *18th Congrès Français de Mécanique*, Grenoble, French, 27-31 August 2007

[5] Kornblum Y., and Goldstein J., Jet impinging on semicircular concave and convex surfaces – Part II: Heat transfer, *The Physics of Heat Transfer in Boiling and Condensation: International Symposium*, Moscow, 21-24 May 1997

[6] Fénot M., Vullierme J.J., and Dorignac E., A heat transfer measurement of jet impingement with high injection temperature, *CR Académie des Sciences*, Vol. 333, No. 10, 2005, pp. 778-782

[7] Brevet P., Dejeu C., Dorignac E., Jolly M. and Vullierme J.J., Heat transfer to a row of impinging jets in consideration of optimization, *International Journal of Heat and Mass Transfer*, Vol. 45, 2002, pp. 4191-4200